Effect of Different Operating Conditions on the Corrosion of Carbon Steel in Oxygenated Sodium Sulphate Solution

Sara A. Sadek & Basim O. Hasan

Chemical Engineering Department, Al-Nahrain University, Iraq

Abstract :

Carbon steel is a major metal used in manufacturing of the equipments used in petroleum industry and it is subject to different operating conditions causing various corrosion attacks. Corrosion of carbon steel in sodium sulphate solution (Na_2SO_4) under flow conditions was investigated using rotating cylinder electrode (RCE) for a range of rotation velocity (0 – 2000 rpm) and temperatures (32 - 52 ^{o}C). The corrosion rate was determined by using both weight loss method and electrochemical polarization technique (limiting current density). Different salt concentrations were investigated ranged from 0.01 to 0.4 M. The effect of time (or corrosion product formation) and the effect of oxygen concentration through air bubbling in the solution were also investigated and discussed. The results showed that increasing rotational velocity leads to a considerable increase in the corrosion rate represented by limiting current density. The corrosion rate had unstable trend with salt concentrations and temperature. Generally, the corrosion rate decreased appreciably with time due to the formation of corrosion product layer depending on rotational velocity, temperature, and oxygen concentration. It was found that, air pumping through the salt solution leads to a considerable increase in the limiting current density (i_L) depending on rotational velocity, temperature, and time.

Keywords: corrosion, carbon steel, sodium sulphate, velocity, oxygen.

1. **Introduction**

In petroleum industry the equipments are subject to corrosive environments causing different operational problems. Studying the corrosion behavior of carbon steel under different operating conditions is of vital importance of petroleum industry. Salts dissolved in water have a marked influence on the corrosivity of water. At extremely low concentrations of dissolved salts, different anions and cations show varying degrees of influence on the corrosivity of the water. The anions most commonly found in water are chloride, sulphate and bicarbonate. There are many investigations for corrosion of carbon steel in neutral aerated salt solutions, especially in sodium chloride (NaCl) solution. Little investigation has been found for corrosion of carbon steel in Na_2SO_4 salt solution. The sulphate ion has a greater effect on the corrosivity of the water than the chloride ion, and the bicarbonate ion shows inhibitive tendencies.   In addition sodium sulphate is presented in considerable concentration in the accompanying water with crude oil causing corrosion for the handing pipelines. Generally corrosion of turbine caused by a thin film deposit of fused salt (sodium sulphate) on alloy surface (carbon steel) is an example of corrosion in sodium sulphate [1, 2]. During combustion in the gas turbine, sulfur from the fuel reacts with sodium chloride from ingested air at elevated temperatures to form sodium sulphate. The sodium sulphate then deposits on the hot-section components, such as nozzle guide vanes and rotary blades, resulting in accelerated oxidation attack [3]. Sodium sulphate also cusses corrosion in boiler that used sodium sulfite (Na_2SO_3) as oxygen scavenger when Na_2SO_3 reacted with oxygen at low temperature and pressure it forms sodium sulphate that causes serious attack to the tubes of the boiler [4]. Despite its relatively limited corrosion resistance, carbon steel is used in large tonnages in marine applications, nuclear power and fossil fuel power plants, transportation, chemical processing, petroleum production and refining,

pipelines, mining, construction and metal-processing equipment [5]. The following reactions occur as the result of the corrosion of carbon steel in sodium sulphate (Na_2SO_4) aqueous solutions [6]:

$$Fe_{(s)} \leftrightarrow Fe^{+2} + 2e^- \qquad\qquad (1)$$

$$SO_4^{-2} + Fe_{(s)} \leftrightarrow Fe\,SO_{4\,(aq)} + 2e^- \qquad\qquad (2)$$
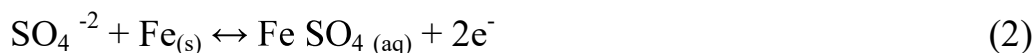
It is well known that the rate controlling step in most natural water corrosion process is the cathodic half reaction. The most important cathodic process in aerated waters is oxygen reduction. The rate of this half reaction is generally limited by the speed at which oxygen can reach the surface of the metal. This oxygen is transported from the bulk water to the surface across the boundary layer by diffusion. The oxygen concentration will vary from a minimum at the surface to bulk concentration at the outside edge of the boundary layer. This results in the concentration gradient and promotes the transport of oxygen [7]. If the corrosion process is under cathodic diffusion control then the flow increases the corrosion rate. This effect generally occurs when an oxidizer is present in small amounts, as is the case for dissolved oxygen in acids or water [8]. The effects of concentration, velocity, and temperature are complex and it will become evident that these factors can frequently outweigh the thermodynamic and kinetic considerations [9]. It is widely recognized that the corrosion of carbon steel in aerated neutral solutions may be accounted for by the anodic reaction as in Eq. (1) and cathodic reaction in presence of oxygen:

$$\tfrac{1}{2}\,O_2 + H_2O + 2e^- \rightarrow 2OH^- \qquad\qquad (3)$$

In general, as the corrosion proceeds, the process becomes more complex due to building up of corrosion products which restrain the oxygen transport to the surface, growth of the surface roughness which increases the momentum

and mass transport between surface and solution, changing physico-chemical properties of the corrosion products; and changing mechanics of flow. The formation of corrosion product layer has a noticeable effect of the corrosion rate of the metal depending on the solution nature and on the temperature and hydrodynamics [10, 11,12].

The aim of this work is to study the influence of velocity, temperature, corrosion products layer (or time) on the corrosion rate and corrosion potential of commercial steel pipe in different concentrations of Na_2SO_4 solutions.

2. **Experimental Work**

Figure (1) shows the experimental apparatus that was used to perform the experimental work. It was composed of stirrer to obtain different rotational velocities, water bath to obtain different solution temperatures, power supply to provide a constant applied voltage between the electrodes, digital ammeter to measure the current, digital voltmeter to measure the potential, variable resistance (rheostat) to control the current flow, electrical connection between cathode (specimen) and the cell. Also, air pump to pump the air through the solution, oxygen meter to measure the solubility of oxygen in solution in ppm, pH meter to monitor the pH of the solution, and conductivity meter to measure the electrical conductivity of the solution. Cylindrical carbon steel specimen was prepared to fit the specimen holder with a surface area having a dimensions of 30 mm long (L), 22 mm inside diameter (d_i), and 25 mm outside diameter (d_o). It serves as a cathode.

Before each experiment, the carbon steel specimen (working electrode) was polished with 120, 180, 220, 400 and 2000 grit silicon carbide paper, washed with brushing by plastic brush with running tap water, immersed in ethanol for 30 second dried with clean tissue, and then dried by using electrical

oven to temperature of about 110 ^{o}C for 10 minute. The specimen then was stored in vacuum desiccator over high activity silica gel until use**.**

In weight loss experiments, after the specimen was kept in the dissector to cool, it then was weighted to nearest 0.1 mg (w_1) by using digital balance of high accuracy (4 decimal places of gram) to measure the weight loss. Then the specimen was exposed to corrosion environment for 4 h. At the end of weight loss experiment,   the specimen was washed by tap water with brushing to remove the corrosion products that formed on the outside surface and then immersed in 10% hydrochloric acid containing chemical inhibitor (thioharnstoff) for 30 second [13,14]. Blank tests showed no appreciable weight loss caused by cleaning with inhibited acidic solution. After that the specimen was washed by tap water, distilled water, dried with clean tissue, rinsed in ethanol and dried by using electrical oven to a temperature about 110 ^{o}C for 10 minutes. Then the specimen was kept in the dissecator to cool and then weighted (w_2). So that the corrosion rate can be determined using:

$$CR = \frac{\Delta W}{A \times t} \tag{4}$$

And the limiting current density can be determined by using the following equation:

$$i_L = z \, F \, N_{O2} \tag{5}$$

N_{O2} is the molar flux of oxygen which is defined as the moles of O_2 reacted per unit area per unit time (gmol/m^2.s). Also, according to reactions 1 and 3, N_{O2} = $0.5 N_{Fe}$.

In polarization experiments, the counter (auxiliary) electrode was made of graphite which serves as anode. The surface area of the counter electrode was made larger than that of the working electrode (Aa/Ac =2.7) to ensure that the

limiting current density occurs on the cathode rather than anode [15, 16]. Salt bridge connected to standard calomel electrode (SCE) was used as reference electrode employed to measure the potentials. The luggin capillary of the reference electrode was placed 2 mm downstream of the working electrode. The electrical connection between the circuit and the rotating specimen was attained by using graphite brush.

To investigate the effect of time on the corrosion rate, in polarization measurements after the solution had reached the desired temperature, the electrical circuit was switched on where maximum current pass through the cell because the resistance equals to zero. The specimen was cathodically polarized from a potential of nearly -1.4 V (vs. SCE) to the corrosion potential (where i_{app} = 0) at a rate of $5 - 10$ mV by changing the applied current using rheostat, i.e. 5 mV when the change of current with potential is high (near corrosion potential) and 10 mV when the change of current with potential is low, i.e. in the limiting current density region. The current was recorded for step changes in potential. Two minutes were allowed for steady state to be reached after each potential increment [11, 15]. For the experiments with air bubbling, the air is pumped using air pump for 15 minutes before each run and the bubbling is kept until the end of the run. The oxygen concentration was measured for each condition using dissolved oxygen meter. After collecting the data by recording the current and potential, polarization curve can be drawn by using semi log scale where the x-axis represents the current density (log scale) and the y-axis represents the potential. So that the limiting current density can be obtained from this curve. Method proposed by Gabe and Makanjoula [16] was adopted to determine the limiting current.

The obtained values of i_L represent values for clean surface (t = 0), i.e. no corrosion products were formed, since during the polarization experiment no free corrosion occurred (except at low currents near the corrosion potential)

because the specimen was cathodically protected. To investigate the influence of time on the instantaneous corrosion rate, the electrical circuit was switched off and the specimen was allowed to corrode freely at a particular velocity and temperature. A free corrosion of the specimen continues for 1 h during this interval corrosion proceeds and the corrosion product forms on the surface of the specimen. At the end of 1 h, the electrical circuit was again switched on and the specimen was polarized to −1.4 V (vs. SCE) and polarization experiment was repeated to obtain the complete polarization curve and new i_L. This value of i_L represents the value at t =1 h. At the end of the second polarization measurement, the electrical circuit was switched off while the specimen was kept corroding in the solution for another 1 h. During this second interval, the specimen will undergo a free corrosion forming additional corrosion products. The specimen was then polarized to −1.4 V (vs. SCE) by switching on the electrical circuit again to repeat the polarization experiment and to obtain new i_L at t =2 h. Each run was carried out in duplicate with third run when the reproducibility was in doubt. The solubility of oxygen at different velocities, temperatures, and salt concentration was measured in ppm at each 15 min using dissolved oxygen meter.

3. <u>Results and Discussions</u>

Figure (2) shows the corrosion rate obtained from weight loss experiments expressed in gmd in 0.2 M Na_2SO_4 versus rotational velocity. From Figure (2) it is clear that increasing flow velocity leads to an increase in corrosion rate. It can be seen that the corrosion rate increases from 26 gmd to 118 gmd (350 %) when the rotational velocity increased from 0 to 2000 rpm. This increasing is due to the increase in oxygen transport toward the surface because the rate of oxygen reduction reaction is generally limited by the speed at which oxygen can reach the surface of the metal. Previous studies [9,11,17,

18] indicated the greater turbulence due to high velocities results in more uniform O_2 concentration near the surface. It is to be noted from Figure (2) that when the rotational increased from 1500 rpm to 2000 there is no increase in the corrosion rate. This the behavior can be interpreted as follows: when the velocity increase, the transport of O_2 increases toward the surface with increasing velocity. At high velocities the rate of oxygen transport to the surface becomes higher or equal to the rate of O2 consumption on the surface, therefore further increase in the velocity has no effect to increase the corrosion rate.

Figures (3-5) show the polarization curve for carbon steel corrosion for different rotational velocities in 0.2 M Na_2SO_4 at 32 , 42 , and 52 ^{o}C respectively. It is clear that the current reaches the limiting value when the potential approaches the H_2 evolution potential. In addition, the higher the velocity is the higher the i_L will be. It should be noted from Figs. 3 to 5 that the limiting current density region is not clear for the case of zero rotational velocity (static conditions), where, th ^{4} larization curve is not too steep and hence the limiting current cannot be obtained, i.e. the polarization technique fails to determine the corrosion rate. This behavior can be reasoned to the fact that for stationary conditions the corrosion potential is relatively low, therefore the limiting current occurs near the hydrogen evolution region. Hence,, no oxygen limiting current appears due to the generation of other reduction reactions currents such as the hydrogen reduction currents. In such cases, the weight loss method must be adopted.   Figure (6) shows the effect of velocity and temperature on i_L, From this figure it is clear that increasing the velocity leads to an increase in the limiting current density. The average increase in the i_L with the velocity for the three temperatures is about 200% for a velocity range from 250 rpm to 2000 rpm. The increase in the i_L because the increase in the transport of oxygen to the metal surface [18, 9].   Examining literature reveals

a variety of i_L dependence on flow velocity that was found by authors for various geometries. The manner in which velocity affects the limiting diffusion current is a marked function of the physical geometry of the system. This dependence depends on the nature of the system under consideration, i.e., geometry, roughness of the surface, viscosity, and temperature [9, 19, 20, 21]. From this figure, it can be seen that the corrosion rate at 42°C is higher than at 32°C and 52 °C; also, the corrosion rate at 52 °C is higher than at 32 °C. The effect of temperature on the corrosion rate for mass transfer control systems is represented by changing two parameters affecting the corrosion rate in conflicting ways that are the O_2 solubility and diffusivity. The corrosion rate at 42 °C is higher than 52 °C can be ascribed to the lower concentration of O_2 at 52°C than 42°C. Increasing the temperature will increase the rate of oxygen diffusion to the metal surface by decreasing the viscosity of water enhancing the corrosion rate. On the other hand, increasing temperature decreases the oxygen solubility the factor that restrains the corrosion [19,22]. Table (1) shows the experimentally measured solubility of oxygen (C_b) in ppm by using oxygen meter at various sodium sulphate concentrations. From the table it is clear that at a given temperature, increasing the dissolved salt (Na_2SO_4) concentration leads to a decrease in the O_2 concentration. Also, the temperature has an effect on the solubility of oxygen at constant salt concentration, that is, increasing the temperature leads to a significant decrease in the O_2 concentration. Table 2 shows the solubility of oxygen (C_b) in 0.2 M Na_2SO_4 solution with air bubbling under different conditions. It is clear that adding air bubbles lead to an increase in the O_2 concentration at constant salt concentration and temperatures, also, increasing velocity leads to an increase in the C_b when pumping the air in the solution because the velocity will increase the turbulence by eddy diffusion and increase the distribution of bubbles within the solution and hence more O_2 transfer to the solution. Also increasing the temperature for a constant salt

concentration and velocity leads to a decrease in C_b because the escape of O_2 from the solution to atmosphere. Figure (7) shows the effect of rotational velocity on the limiting current density in presence of air bubbling. Comparing Figure (7) with Figure (6) indicates that adding air bubbles to the electrolytic solution leads to an increase in the i_L (the corrosion rate) for certain temperature and velocity due to the increased O_2 concentration. The Figure (7) reveals that, for all velocities, i_L at 42 $^{\circ}$C is higher than that at 32 $^{\circ}$C and 52 $^{\circ}$C. Also i_L at 52 $^{\circ}$C is higher than 32 $^{\circ}$C. This behavior of corrosion rates indicates that the combined effect of O_2 solubility and molecular diffusivity is highest at 42 $^{\circ}$C followed by 52 $^{\circ}$C and 32 $^{\circ}$C, i.e. at 42 $^{\circ}$C the effect of these two parameters on the corrosion rate is maximum. The increase in corrosion rate when the velocity increased from 250 rpm to 2000 rpm in presence of air bubbles is 420% at 32 $^{\circ}$C, 260% at 42 $^{\circ}$C, and 450% at 52 $^{\circ}$C. Comparing these values with that in Figure (6) (no O_2 bubbling) indicates that the presence of O_2 leads to appreciable increase in the effect of velocity on the corrosion rate. Figure (8) shows the experimentally measured electrical conductivity of the solution for different salt concentrations at various temperatures using digital electrical conductivity meter. It is clear that increasing salt concentration leads to an increase in the conductivity of the solution at constant temperature. Also, the higher the temperature is the higher conductivity will be. Figure (9) shows the effect of sodium sulphate concentrations on the i_L at 750 rpm. It is clear that increasing Na_2SO_4 concentration from 0.01 to 0.1 M leads to an increase in i_L from 5.75 to 9 A/m^2 (56%) at 32 $^{\circ}$C, from 9 to 12.5 A/m^2 (40%) at 42 $^{\circ}$C, and from 7.75 to 11 A/m^2 (42%) at 52 $^{\circ}$C. Beyond this concentration, the i_L shows a considerable decrease at all temperatures. This behavior can be attributed to the increased electro-conductivity because of the increased salt content, until the salt concentration is great enough to cause an appreciable decrease in the oxygen solubility, resulting in a decrease in the rate of depolarization. The same

trend was noticed in previous works for corrosion in NaCl solution [23]. Peralta et al. [6] stated that the mechanism of corrosion attack in sulphate solutions occurring on the surface of the mild steel after a certain exposure can be regarded as partially uniform. This attack started in isolated locations and spread laterally without developing any pits. The effect of SO_4^{-2} on the rate of oxidation of iron in mildly alkaline solutions results from its ability to form soluble complexes with Fe^{+2} or Fe^{+3} ions. Also, it is found that sulphate ions accelerate the active dissolution of iron and the films formed in sulfate solutions resulted from supersaturated solutions of iron salts, most probably iron hydroxysulfate. This implies that iron dissolves in sulphate solutions at a high rate, creating a supersaturated solution and allowing precipitation of a non protective film . Figure (10) shows the polarization curves for u = 250 rpm at temperature of 32 ^{o}C and in 0.2 M Na_2SO_4 solution at different time intervals. It is evident that the i_L decreases with time due to the continuous growth of the corrosion product layer (fouling layer) which decreases the transport of O_2 to metal surface and the activity of the surface and hence the corrosion rate [19, 24]. Figure (11) shows the effect of time on the i_L at the three temperatures for velocity of 250 rpm. It can be seen from this figure that the i_L decreases with time for the three temperature. The highest decrease is in the case of T=42 ^{o}C which is up to 55 % after 2 h. The decrease in the corrosion rates in 32 ^{o}C and 52 C are 45% and 40% respectively. At time zero, where no corrosion products are found, the corrosion rate (i_L) at 42 ^{o}C is highest, while, at 32 ^{o}C and 52 ^{o}C, the corrosion rates are comparable. At times of 1 h and 2 h, the corrosion rate of 32 ^{o}C still lower but the corrosion rates at 42 ^{o}C and 52 ^{o}C are comparable. This trend indicates that the effect of corrosion product formation (fouling) to decrease the corrosion rate is highest at 42 ^{o}C. Also, the rise in temperature contributes to increase the porosity (or decrease the density) of corrosion products layer and that facilitates the passage of O_2 toward the surface [11, 19].

That is why the effect of corrosion products to decrease the corrosion rate at 32 ^{o}C and 42 ^{o}C is higher than in 52 ^{o}C. Figure (12) shows the effect of time on the i_L at the three different velocities 250, 1000, 2000 rpm at temperature of 32 ^{o}C. The figure indicates that the formation of corrosion products with time decreases i_L for all values of velocity. It can be noted that for low u, i_L slightly decreases with time. As u increases, the decrease in i_L with time becomes higher at first time interval (after 1 h.). After 2 h the decrease is slight. The decrease in the corrosion rate (i.e. i_L) with time for velocity of 250 rpm is about 30%, for 1000 rpm is 35%, for 2000 rpm is 55%. Hence, the higher the velocity is the higher the decrease in the corrosion rate due to high amount of corrosion products formed which in turn restrains the arrival of dissolved O_2 to the surface. This indicates the important inhibitive effect of this fouling layer to decrease the corrosion. Examining literature findings reveals that there are different trends of corrosion rate with formation of corrosion product. The studies of Mahato et. al., [12, 19, 25] for pipe flow, indicated that the corrosion rate always decreases with time. Slaiman and Hasan [11] for pipe flow noticed that at low temperatures the formation of corrosion product leads to a decrease in the corrosion rates even at high velocities, but at high temperature and high flow velocities, the formation of corrosion product leads to increase the corrosion rate. Figure (13) shows the effect of time on the i_L at the three temperatures for velocity of 250 rpm with air bubbling. The figure reveals that at 32 ^{o}C, i_L decreases with time due to the formation of corrosion product. While for high temperature 42 ^{o}C and 52 ^{o}C, i_L steeply decreases at first hour then it has slight decrease with time because of the corrosion rate is higher at first hour than second hour . Figure 14 shows the effect of time on the i_L at the three velocities (250, 750, 2000 rpm) at temperature of 32 ^{o}C in presence of air bubbles. Figure (14) shows the same behavior of i_L with time at different

velocities as in figure (13) but with a significant increase in the exchange current density due to addition of air bubbles.

Figures (15-17) show comparison of the variation of i_L with time in presence and absence of air bubling. It is evident that the bubbling has noticeabl effect on the corrosion rate (i_L) for all temperatures. The corrosion rate at 32 ^{o}C exhibits highest increase of i_L with air bubbling where it ranges from 10 percent at time zero to 50 percent at time 2 h. Howerver, the other two temperatures give lower increase in the corrosion rate, i.e for 42 ^{o}C the increase ranges from 10 pecent to 15 and, for 52 ^{o}C it ranges from 16 percent to 10 percent. The behavior can be interpreted in reference to Table 1 where the increase in O_2 solubility with air bubbling is highest for 42°C causing highest increase in the corrosion rate. Figure (18) shows the effect of rotational velocity on the corrosion potential in 0.2M Na_2SO_4 solution. Figure (19) shows the effect of velocity and temperature on the corrosion potential (E_c) in 0.2 M Na_2SO_4 in presence of air bubbles. In both figures, it is clear that the corrosion potential is shifted to more positive values with increasing rotation velocity. In addition there is considerable increase of E_c with the temperature in case of air bubbling Figure (19). This indicates that the high concentration of O_2 leads to an increase in the effect of temperature on E_c. Therefore, the corrosion potential in aerated and oxygen-saturated solutions is flow dependent since the cathodic process, i.e., oxygen reduction reaction, is mass transfer controlled. This behavior is in agreement with previous findings [26, 27, 24, 28]. Ross et. al. [29] stated that the increase in E_c with velocity is due to the increase in oxygen transport to the metal surface and when the system is free from oxygen, the velocity has no effect on E_c.

Conclusions :

The corrosion rate of carbon steel represented by limiting current density in sodium sulphate increases with increasing rotation velocity and have complex trend with temperature and oxygen concentration. For the range of temperature from 32 to 52 ^{o}C, the corrosion rate increases three times (as an average) when the rotational velocity increases from 0 to 2000 rpm. When air is bubbled in Na_2SO_4 solution the O_2 concentration increases slightly causing an appreciable increase in the corrosion rate. The consequent increase in the corrosion rate ranges from 10% percent to 50% depending on the rotational velocity and solution temperature. In addition, the increase in the O_2 concentration shifts the corrosion potential considerably to more positive direction. The corrosion rate at 42 ^{o}C is higher than that at 32 ^{o}C and 52 ^{o}C in presence and absence of air bubbles. The corrosion rate increases by 40% to 55% , depending on the temperature, with increasing Na_2SO_4 concentrations up to 0.1 M and then the it decreases mainly due to the decrease in O_2 concentration with further increase in Na_2SO_4 concentration. The time has a noticeable effect on the corrosion rate due to the formation of corrosion product layer (fouling layer). The formation of this layer causes reduction in corrosion rate by 40% to 55% depending on the temperature and rotational velocity. For the case of air bubbling at 32 ^{o}C, the reduction in the corrosion rate with time ranges between 30% to 55% indicating that this layer plays important role in corrosion mitigation corrosion.

References:

1. Bornstein N. S. and M. A. Decrescente, Metall. Trans. 2, 2875 (1971).

2. Goebel J. A, F. S. Pettit and G. W. Goward, "Oxygen Scavengers" Metall. Trans., 4, 261 (1973).

3. Stringer J., "Hot Corrosion in Gas Turbines," ASM International, High Temperature Corrosion and Materials Application, chapter 9, pp. 249-258, 2007

4. Huijbregts W., "Acid Corrosion Resistance of Boiler Steels." Materials Performance. pp. 23-27, 2007.

5. Fouda A.S., G.Y. Elewady and M. N. El-Haddad, "Corrosion Inhibition of Carbon Steel in Acidic Solution Using Some Azodyes" Canadian Journal on Scientific and Industrial Research Vol. 2, No. 1, January 2011.

6. Peralta S. A., J. G. Llongueras , M. P. Pardavé & M. R. Romo, "Study of the electrochemical behaviour of a carbon steel electrode in sodium sulfate aqueous solutions using electrochemical impedance spectroscopy", Journal of Solid State Electrochemistry Springer-Verlag, May 2002.

7. Smith S. W., K.M. McCabe, and D. W. Black 'Effect of Flow Parameters on the Cathodic Protection of A steel Plate in Natural Seawater", Corrosion, vol. 45, No.10, pp.790- 793 October 1989.

8. Shreir L.L., R.A. Jarman & G.T. Burstein "Corrosion Metal / Environment Reactions" third   edition, published by Butterworth-Heinemann Volume I, Great Britain, 2000.

9. Brodkey, R. S. and H. C. Hershey, "Transport Phenomena", second edition, McGraw Hill, New York, 2007.

10. Slaiman Q. J. M. and Basim O. Hasan "Study on Corrosion Rate of Carbon Steel Pipe under Turbulent Flow Conditions" The Canadian Journal of Chemical Engineering Volume 88, December 2010.

11. Mahato, B. K., F. R. Stewrd and L. W. Shimlit, "Steel Pipe Corrosion under Flow Condition—II. Mass Transfer Correlations with Temperature Effects," Corrs. Sci. J. 8, 737–749, 1968.

12. Fontana M.G. and N. D. Greene "Corrosion Engineering", 3rd edition, McGrawHall, London 1986.

13. Hasan, B. O., "Heat, Mass, and Momentum Analogies to Estimate Corrosion Rates under Turbulent Flow Conditions" Ph. D. Thesis Dept. of Chem. Eng., University of AL-Nahrain, Baghdad, 2003.

14. Pickett, D. J. and K. L. Ong, "The Influence of Hydrodynamic and Mass Transfer Entrance Effects on the Operation of a Parallel Plate Electrochemical Cell," Electchmica Acta 19, 875–881, 1974.

15. Gabe D.R. and P.A. Makanjoula, EFCF Publication Series No. 15, Electrochemical Eng., AICHE Symposium Series, No. 98, P.309, 1986.

16. Evans, U. R. and T. P. Haoar, "Electrochemical Mechanism of Atmospheric Rusting," Proc. R. Soc. Lond. Ser. A 137, 343, 1932.

17. Foroulis Z. A. "The Influence of Velocity and Dissolved Oxygen on the Initial Corrosion Behavior of Iron in High Purity Water", Corrosion, Vol. 35, P. 340344, 1979.

18. Mahato, B. K., C. Y. Cha and W. Shemlit, "Unsteady State Mass Transfer Coefficients Controlling Steel Pipe Corrosion under Isothermal Flow Conditions," Corros. Sci. 20, 421–441, 1980.

19. Poulson, B., ''Electrochemical Measurements in Flowing Solutions,'' Corrosion Sci. **23**, 1, 391–408 (1983).

20. Stern M., ''Fundamentals Electrode Processes in Corrosion,'' Corrosion-NACE **13**, 97–104 (1957).

21. Henry S.D and W.M. Scott "Corrosion in the Petrochemical Industry", 1st edition, ASM International, USA, 1999.

22.23-Revie R.W. and H. H. Uhlig, "Corrosion and Corrosion Control an Introduction to Corrosion Science and Engineering" fourth edition, published by John Wiley & Sons, Inc., Hoboken New Jersey, 2008.

23.24-Makrides, A.C., J. Electrochem. Soc., vol. 107, P. 869, 1960.

24.25- Mahato, B. K., S. K. Voora $_8$ ˙ L. W. Shemilt, "Steel Pipe Corrosion under Flow Condition—an Isothermal Correlation for a Mass Transfer Model," Corros. Sci. 8, 173–193, 1968.

25.26-Hubbard, D. W. and E. N. Lightfoot, "Correlation of Heat and Mass Transfer Data for High Schmidt and Reynolds Numbers", Ind. Eng. Chem. 5, 370–379, 1966.

26.27-Nesic, N., B.F.M. Pots, J. Postlethwaite, and N. Trevenot, J. Corrosion Science and Eng., Ph. D. Study, Vol.1, Paper 3, 1995.

27.28-Chin, R.J., and K. Nobe, "Electrochemical aspects of Steel Corrosion in Sea Water", Corrosion J., Vol.33, P.364, 1977.

28.29-Ross, T.K., G.C. Wood, and I. J. Mahmud, "The Anodic Behavior of Iron Carbon Alloy in Moving Acid Media" Electrochem. Soc., Vol. 113, P.334, 1996.

Nomenclature:

A: the area = $\pi * d_o * L$ in m^2.

D: Diffusivity (m^2/s)

Ec: corrosion Potential (V)

t: time of exposure (hours)

V: Volts

ΔW: the weight loss = $w_1 - w_2$ in grams.

i_L :   limiting current density in A/m^2.

i_c : corrosion current density, A/m^2

z: number of electron freed by corrosion reaction

     (z for iron is 2 and for oxygen is 4).

F: Faradays constant (96487 columb/equivalent).

C_b: the solubility of oxygen in ($mole/m^3$).

CR: corrosion rate

rpm: revolution per minute.

u: rotational velocity in rpm.

N_{O2}: molar flux ($mole/m^2.s$).

μ: viscosity in $Kg/m.sec^2$.

ρ: density in kg/m^3.

Table 1: measured oxygen solubility in ppm at different sodium sulphate concentrations

Na$_2$SO$_4$ concentrations in M	C$_b$, ppm		
	32 ℃	42 ℃	52 ℃
0.4	5.9	5.08	4.72
0.2	6.2	5.32	4.94
0.1	6.51	5.58	5.17
0.05	6.85	5.84	5.41
0.025	7.19	6.12	5.67
0.01	7.56	6.41	5.93

Table 2: measured oxygen solubility in ppm (mg/L) in 0.2 M Na$_2$SO$_4$ with addition of air bubbles.

u rpm / T ℃	C$_b$ ppm		
	32℃	42℃	52℃
0	7.34	6.54	5.97
250	9.01	8.05	6.21
750	10.5	8.21	6.58
2000	12	8.89	6.95
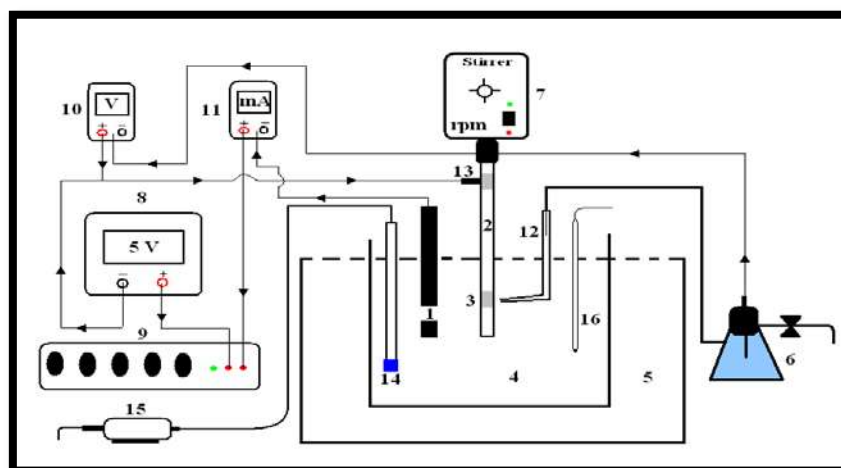
Fig. (1) Experimental apparatus.

1- graphite electrode (anode), 2- rotating shaft (holder), 3- working electrode (specimen), 4- beaker , 5- water bath, 6- calomel electrode (reference electrode), 7- stirrer, 8- power supply, 9- resistance box, 10- voltmeter, 11-ammeter, 12- Luggin capillary, 13- brush 14- air distributer, 15- air pump, 16-thermometer.
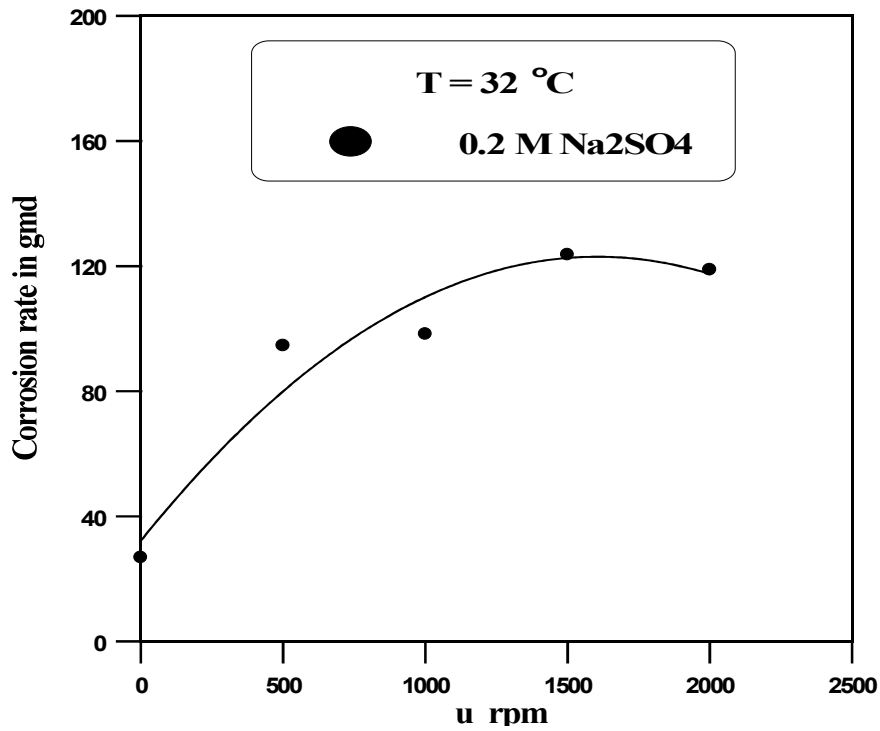
Fig. (2) Corrosion rate in 0.2 M Na₂SO₄ solution versus velocity at 32 ᵒC
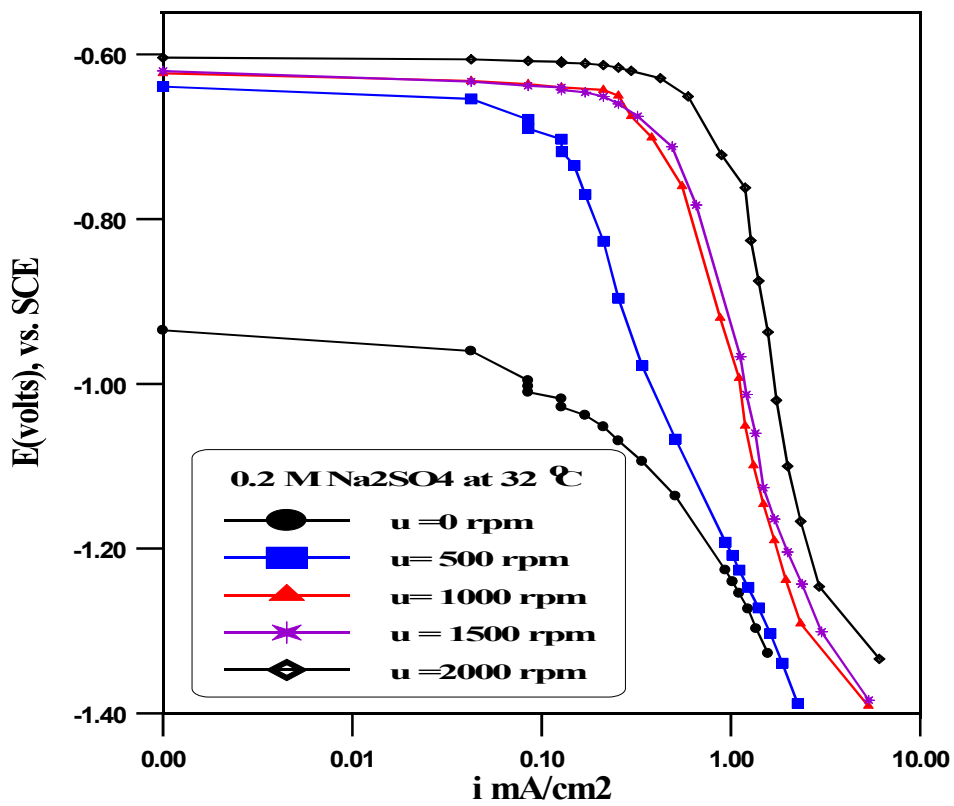
Fig. (3) Polarization curve at different velocity and 32 ᵒC.
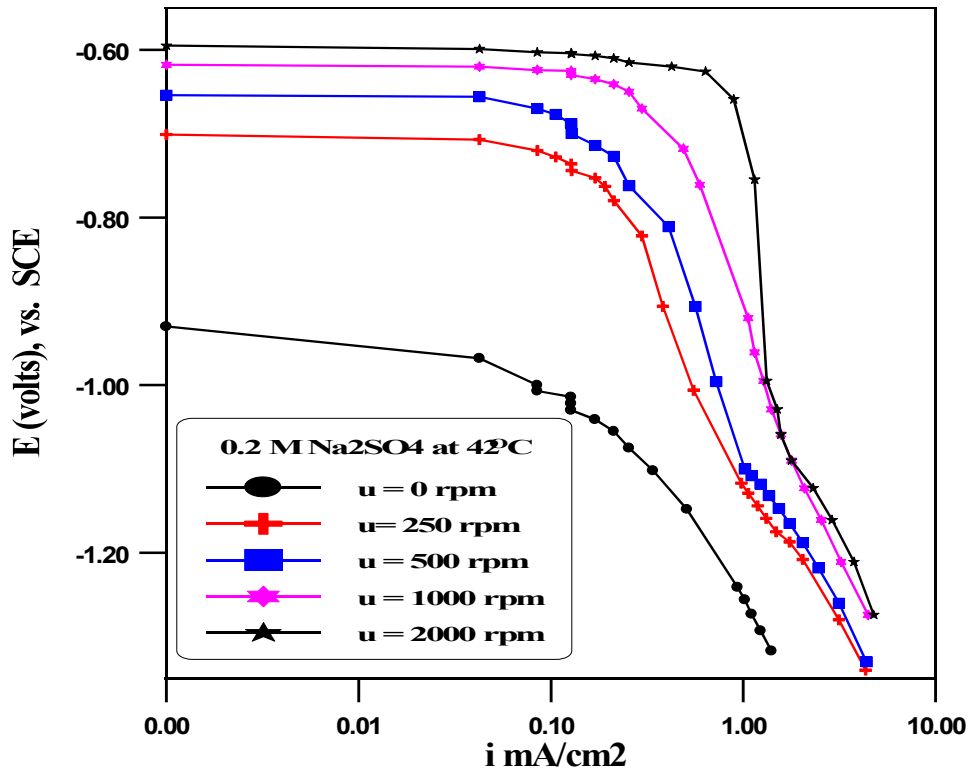
Fig. (4) Polarization curve at different Velocity and 42 ^{o}C
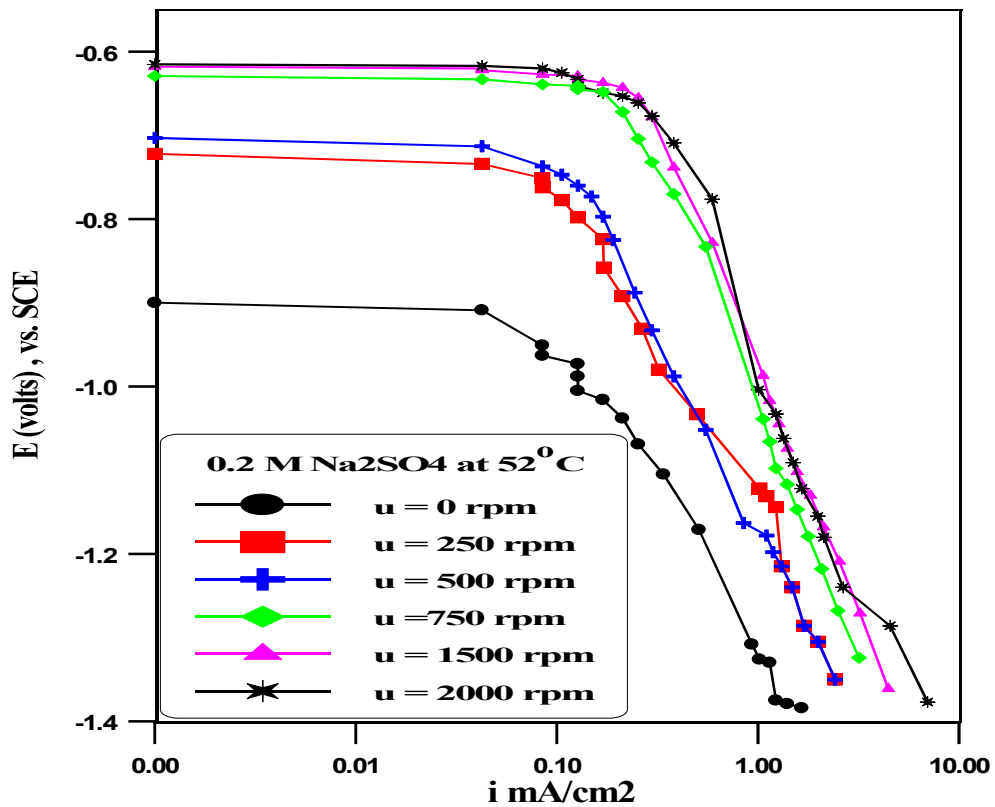
Fig. (5) Polarization curve at different Velocity and 52 ^{o}C
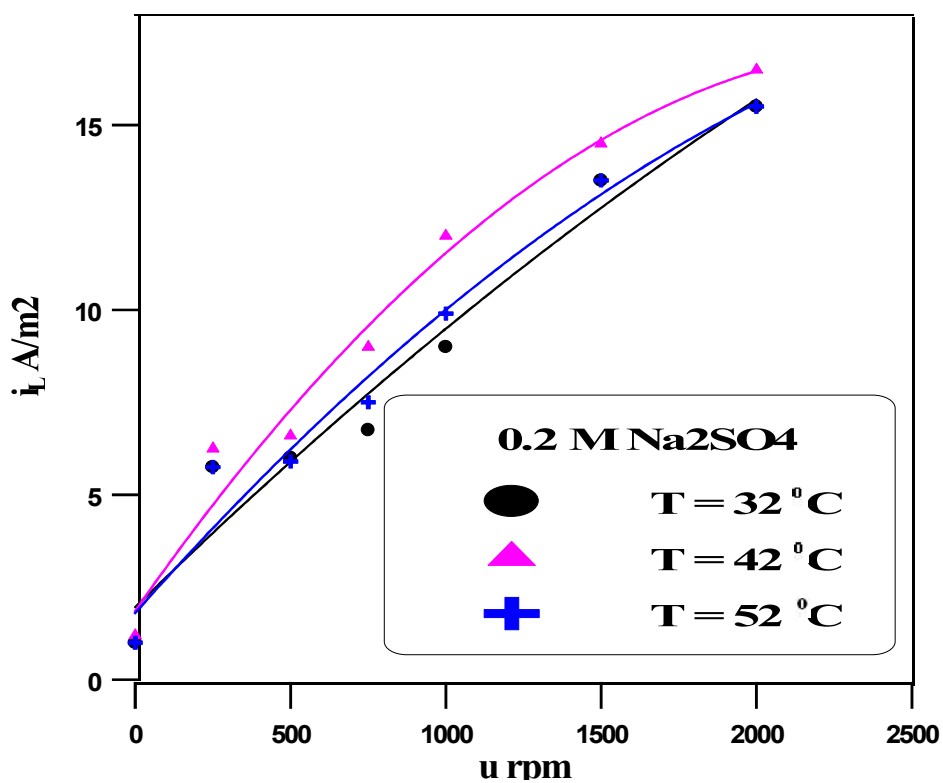
Fig. (6) Effect of velocity and temperature on i_L .
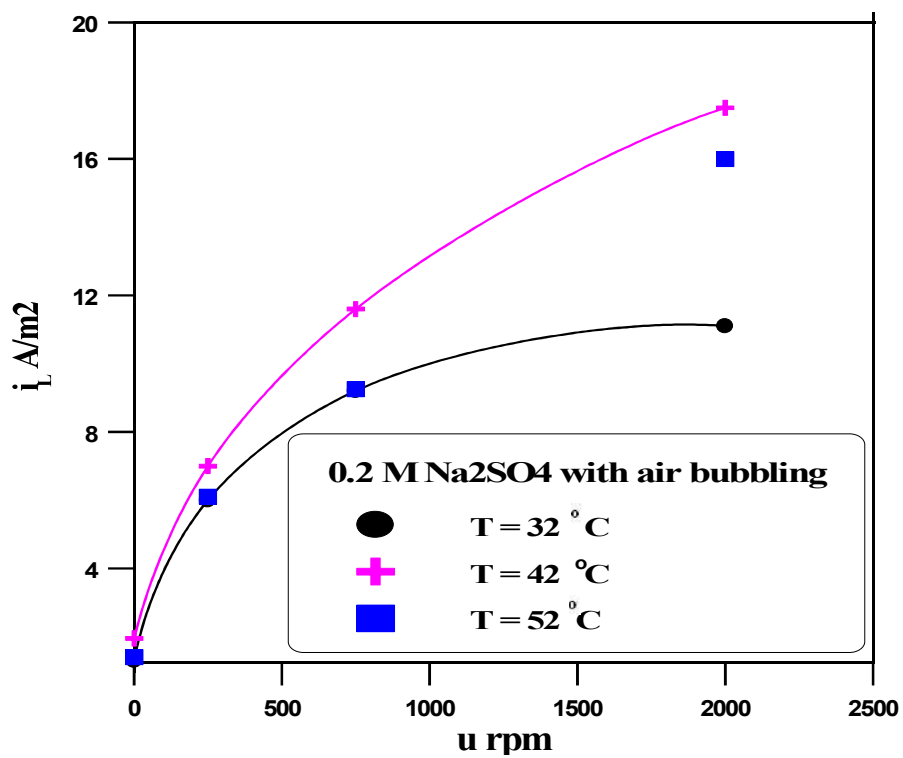
Fig. (7) Effect of velocity on i_L with air bubbling at different temperatures
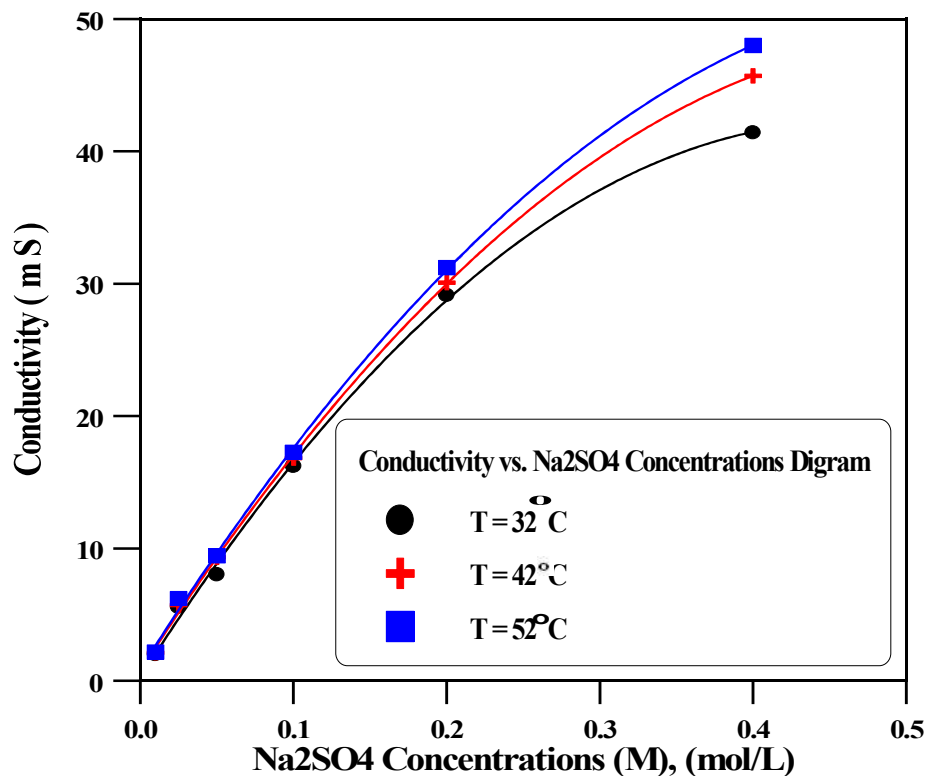
Fig. (8) Conductivity versus Na$_2$SO$_4$ concentrations.
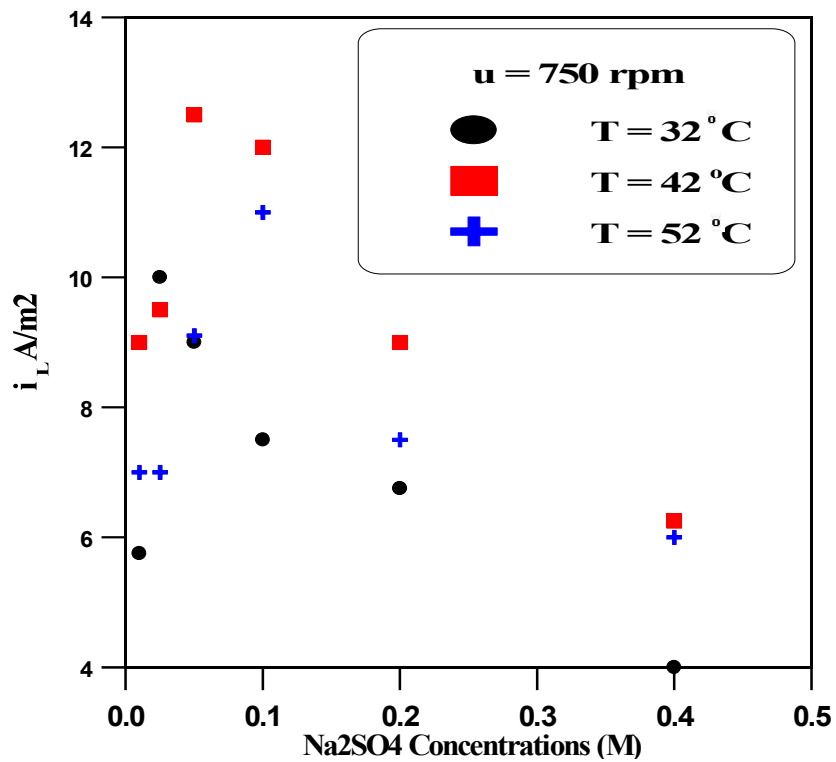
Fig. (9) Effect of different concentration of Na$_2$SO$_4$ and temperatures on i$_L$ at 750 rpm.
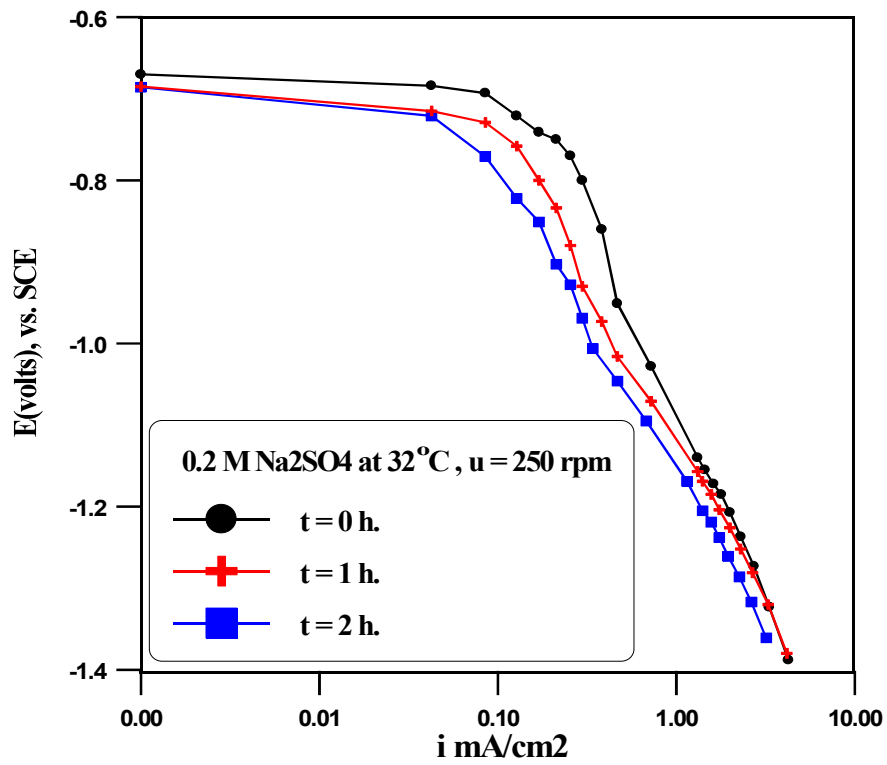
Fig. (10) Polarization curve at u = 250 rpm and 32 ^{o}C in 0.2 M Na$_2$SO$_4$ solution at different time intervals.
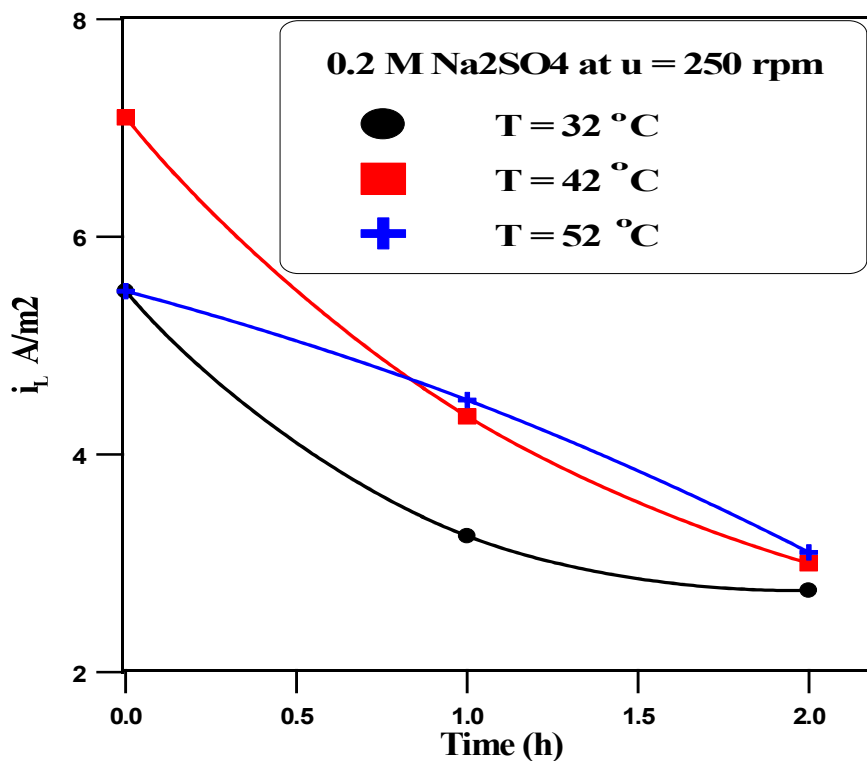
Fig. (11) Effect of time on the i$_L$ at the three temperatures with velocity 250 rpm
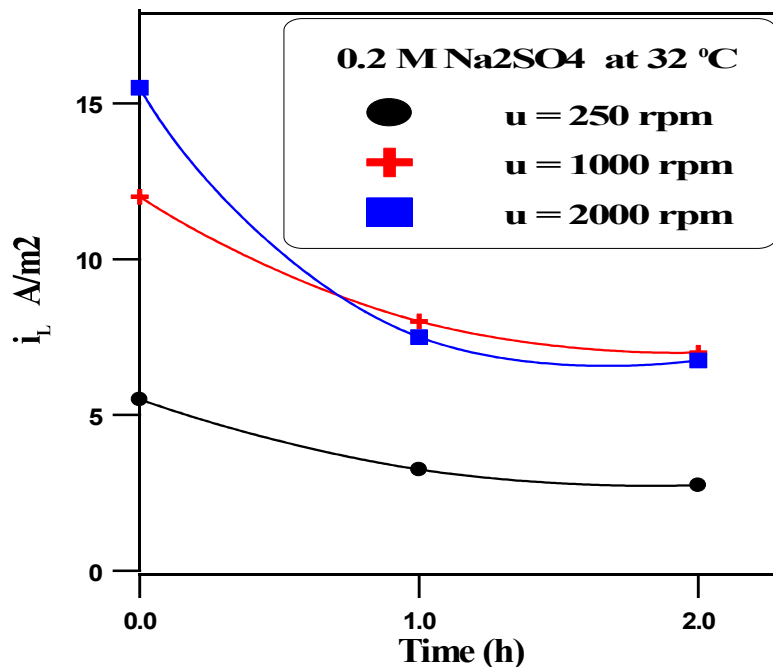
Fig. (12) Effect of time on i_L at three velocities at 32 ^{o}C.
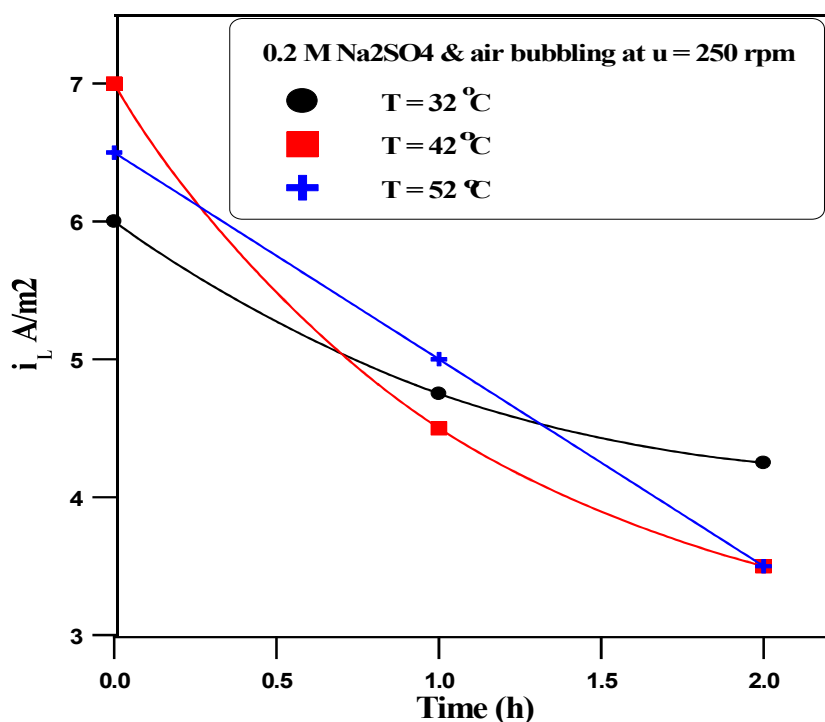
Fig. (13) Effect of time on i_L at 250 rpm and different tempreatures with air bubbling
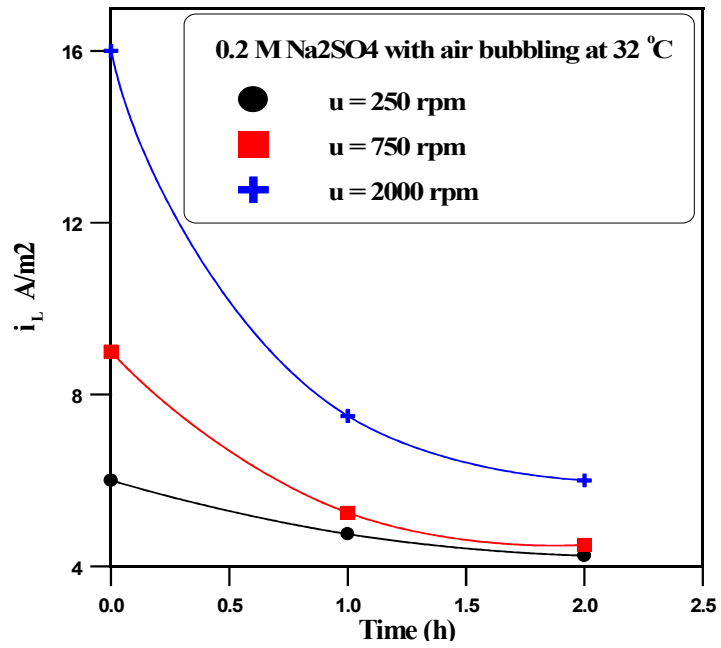
Fig. (14) Effect of time on i_L at 32°C and different velocities.
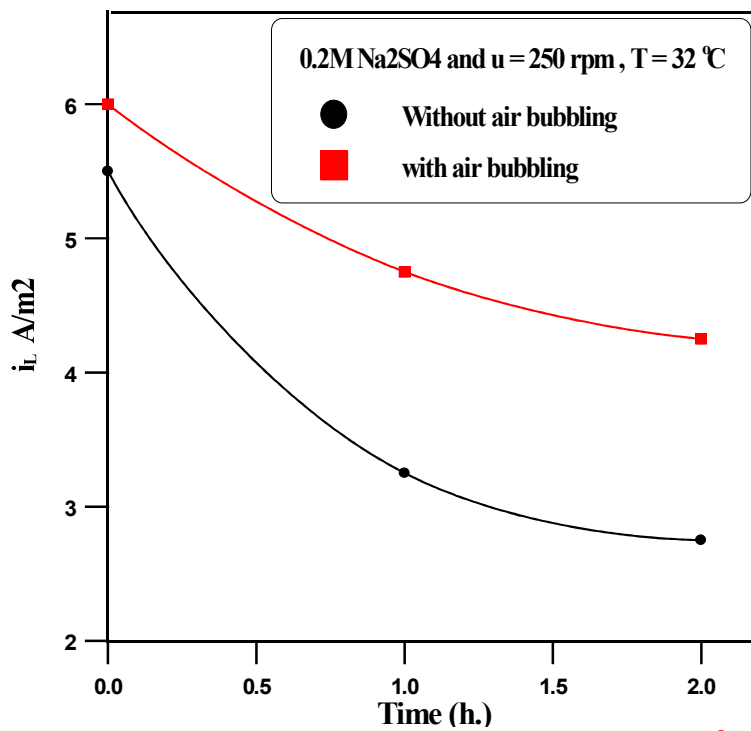
Fig. (15) i_L vs. .time with and without using air bubbles at 32°C and 250 rpm.
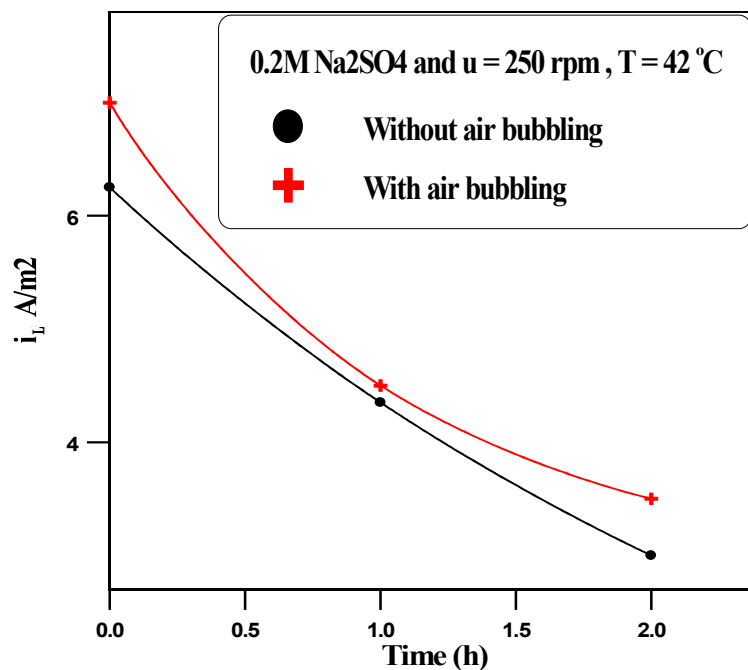
Fig. (16) Variation of i_L vs. time with and without using air bubbles at 42°C & 250 rpm
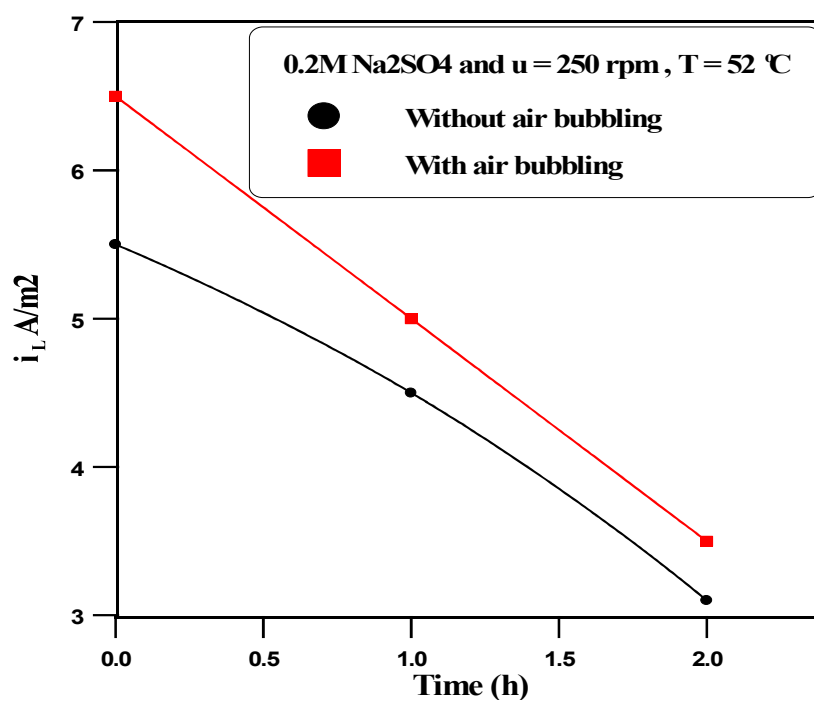

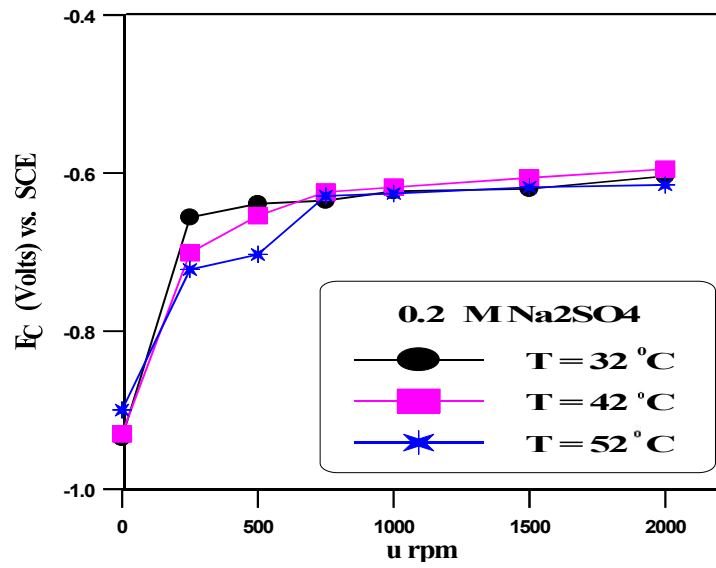**Fig. (17) i_L vs. time with and without air bubbling at 52°C and 250 rpm**

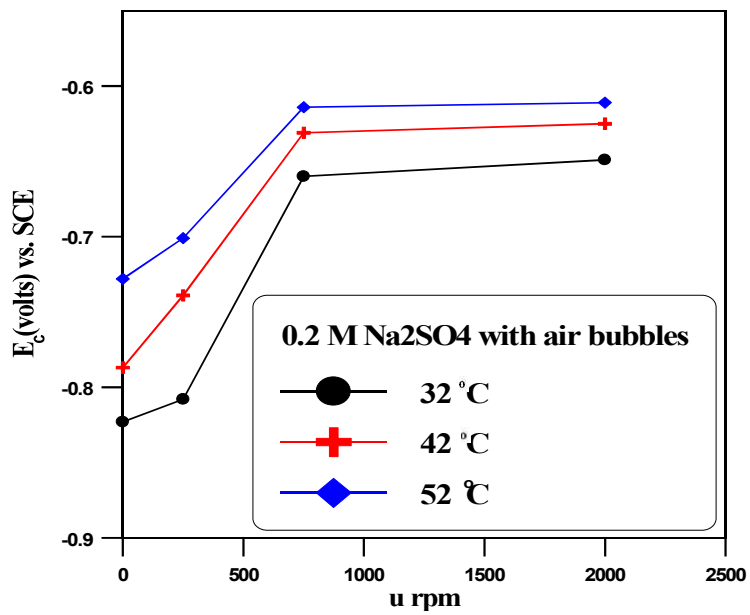**Fig. (18) Ec vs. velocity in 0.2 M Na$_2$SO$_4$ at different temperatures.**

Fig. (19) E$_c$ vs. velocity at different temperatures with air bubbles.